Gaussian memory in kinematic matrix theory for self-propellers

Amir Nourhani,[1,*] Vincent H. Crespi,[1,2,3] and Paul E. Lammert[1]
[1]*Department of Physics, The Pennsylvania State University, University Park, Pennsylvania 16802, USA*
[2]*Department of Materials Science and Engineering, The Pennsylvania State University, University Park, Pennsylvania 16802, USA*
[3]*Department of Chemistry, The Pennsylvania State University, University Park, Pennsylvania 16802, USA*
(Received 5 September 2014; published 4 December 2014)

We extend the kinematic matrix ("kinematrix") formalism [Phys. Rev. E **89**, 062304 (2014).], which via simple matrix algebra accesses ensemble properties of self-propellers influenced by uncorrelated noise, to treat Gaussian correlated noises. This extension brings into reach many real-world biological and biomimetic self-propellers for which inertia is significant. Applying the formalism, we analyze in detail ensemble behaviors of a 2D self-propeller with velocity fluctuations and orientation evolution driven by an Ornstein-Uhlenbeck process. On the basis of exact results, a variety of dynamical regimes determined by the inertial, speed-fluctuation, orientational diffusion, and emergent disorientation time scales are delineated and discussed.

DOI: 10.1103/PhysRevE.90.062304 PACS number(s): 82.45.−h, 47.63.mf, 05.40.−a, 82.70.Dd

I. INTRODUCTION

Self-propellers with active stochastic dynamics are motile non-equilibrium systems [1–4] ranging from bacteria [5–9], cells [10–20], and nanomotors [21–25] at the microscale to insects [26–28], fishes [29–32], and other animals [33–37], as well as humans [38] and traffic [39] at the macroscale. The variety of stochastic fluctuations and their coupling with self-propellers' deterministic motion leads to distinct dynamical and spreading features (see Fig. 1). Phenomenological modeling of self-propellers' ensemble behavior within the differential-equation based Langevin or Fokker-Planck formalisms grows mathematically cumbersome as the number of distinct elementary contributions to the dynamics grows. To overcome this difficulty, we recently described a kinematic matrix theory for self-propellers with uncorrelated (i.e., white-noise) stochastic dynamics [40]. Here we advance this theory to include *correlated* Gaussian fluctuations—colored noise. We demonstrate the formalism's utility by analyzing a rectilinear self-propeller with velocity fluctuations and orientational inertia and discuss the interplay of finite correlation times of the involved noises, leading to an emergent disorientation time scale and a variety of dynamical regimes.

The dynamics of a self-propeller can decompose into elementary processes such as deterministic translation and rotation as well as stochastic orientational diffusion, flips, and tumbles. In the white-noise limit of the kinematic matrix theory, the kinematic properties of these elementary processes are coded into a matrix, called the *kinematrix*, from which many ensemble properties of the self-propeller can be obtained by simple matrix algebra. This approach reveals universalities in self-propeller behavior that were previously hidden behind the complexity of differential-equation-based approaches [40]. The approximation of a negligible stochastic correlation time has been used extensively to model self-propellers [1,40–48]. However, many physical systems suffer environmental noise in the form of forces that act directly on generalized momenta. Such noise is filtered through the *inertia* of the system and thus becomes colored [49–52]. Invoking the Central Limit Theorem, we can reasonably expect a large fraction of such noises to be approximately Gaussian. Persistence of behaviors in living organisms can also play the role of inertia in a mathematical description, even though it is not genuine mechanical inertia. The term "inertia" should thus be understood in this broad sense. Systems with negligible inertia are special cases included in the formalism, which sheds light on how significant the effects of even a little inertia might be.

In this paper, first in Sec. II we advance the kinematrix approach to include Gaussian noise with finite correlation time, yielding Eqs. (3)–(9). This extended kinematrix formalism again circumvents the need for probability distributions; it also makes the calculations significantly easier by extracting the necessary information solely from the autocorrelation of the correlated noise. Section III then provides an application of the theory, to rectilinear self-propellers with fluctuating engines to study the effects of orientational Gaussian memory (modeled by an Ornstein-Uhlenbeck process) in producing a variety of ensemble regimes.

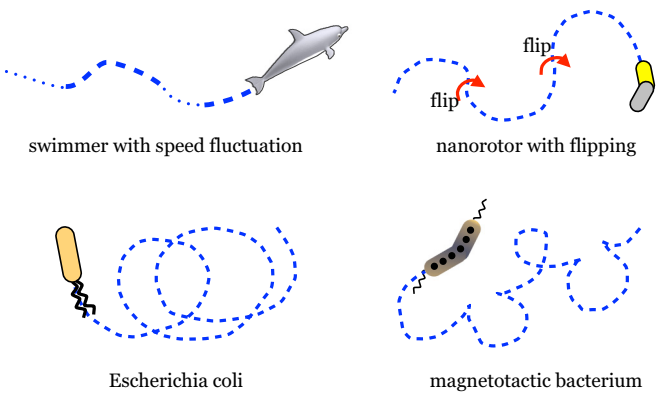

FIG. 1. (Color online) The coupling of deterministic and stochastic elements can give rise to many kinds of distinctive motion and spreading patterns, such as a rectilinear swimmer with speed fluctuation [13,53] and persistent turning [31,32], a nanorotor with flipping [42], E. coli circle swimming [7,54] or magnetotactic bacteria with occasional velocity reversal [55–58].

*nourhani@psu.edu

II. THEORY

The kinematrix formalism is based on an examination of elementary dynamical processes in a self-propeller's body frame. The tail-to-head vector $\boldsymbol{\chi}$ of the swimmer which has a fixed orientation $\hat{\chi}$ in the body frame of the self-propeller evolves with time in the laboratory frame such that, for a given realization of noise, we have at time t the updated value $\hat{\chi}(t) = U(0,t)\hat{\chi}(0)$. The propagator $U(0,t)$ represents the net rotation of the body frame from time 0 to time t; its ensemble average gives the velocity pair correlator of Eq. (6) and the ensemble-average spatial displacement quantities of Eqs. (7)–(9).

To obtain $\langle U(0,t)\rangle$ we work on a discrete timeline $\mathbb{T} = \{0, dt, 2\,dt, 3\,dt, \ldots\}$ with infinitesimal time steps $dt \ll t$. We write U_n for $U(0, n\,dt)$ and $\mathcal{R}_n$ for the net rotation between $n\,dt$ and $(n+1)\,dt$ in the laboratory frame; in the body frame, the same rotation is expressed as $\tilde{\mathcal{R}}_n = U_n^{-1}\mathcal{R}_n U_n$. Rewriting the recursive expression $U_n = \mathcal{R}_{n-1}U_{n-1}$ in terms of the body frame thus yields

$$\langle U_n\rangle = \langle \tilde{\mathcal{R}}_0\tilde{\mathcal{R}}_1\cdots\tilde{\mathcal{R}}_{n-1}\rangle, \tag{1}$$

where the brackets average over all possible realization of noises. If the body-frame rotations $\tilde{\mathcal{R}}_n$ are independent (the white-noise limit) then the average of their product in Eq. (1) is equal to the product of their averages. Then the expansion $\langle\tilde{\mathcal{R}}_i\rangle = \mathcal{I} - \mathcal{K}\,dt + \mathcal{O}(dt^2)$ yields $\langle U(0,t)\rangle = \exp(-\mathcal{K}t)$ where the kinematrix $\mathcal{K}$ captures the kinematic properties of the elementary motile processes [40].

However, for correlated noise the $\tilde{\mathcal{R}}_n$'s are not independent. Assuming physically distinct and independent correlated and uncorrelated noises, we write the rotation $\mathcal{R}_n = \tilde{\mathcal{R}}_n^{\text{corr}}\tilde{\mathcal{R}}_n^{\text{uncr}}$ as the product of correlated $\tilde{\mathcal{R}}_n^{\text{corr}}$ and uncorrelated $\tilde{\mathcal{R}}_n^{\text{uncr}}$ rotations (these being for an infinitesimal interval, the ordering of the rotations makes a negligible difference). Thus, $\langle U_{n+1}\rangle = \langle U_n\tilde{\mathcal{R}}_n^{\text{corr}}\rangle\langle\tilde{\mathcal{R}}_n^{\text{uncr}}\rangle$. The incremental correlated rotation can be written in the form $\tilde{\mathcal{R}}_n^{\text{corr}} = \exp(\boldsymbol{\xi}_n\,dt\cdot\boldsymbol{\mathcal{J}})$, where the $\mathcal{J}_\alpha$ are the generators of rotations in $SO(3)$ (Greek subscripts or superscripts denote Cartesian components x, y, and z). $\{\boldsymbol{\xi}_n\}$ is assumed to comprise a stationary centered Gaussian process with a continuous covariance: $\langle\boldsymbol{\xi}_n\rangle = 0$ and $\langle\xi_n^\alpha\xi_m^\beta\rangle$ is a continuous function of $(n-m)dt$. Expanding the exponential $\exp(\boldsymbol{\xi}_n\,dt\cdot\boldsymbol{\mathcal{J}})$ and expanding uncorrelated rotations to $\mathcal{O}(dt)$ as $\langle\tilde{\mathcal{R}}_n^{\text{uncr}}\rangle \simeq \mathcal{I} - \mathcal{K}^{\text{uncr}}\,dt$ ($\mathcal{K}^{\text{uncr}}$ is the kinematrix of the uncorrelated elementary processes), we obtain

$$\langle U_{n+1}\rangle = \langle U_n\rangle - \langle U_n\rangle\mathcal{K}^{\text{uncr}}dt + \langle U_n(\boldsymbol{\xi}_n\cdot\boldsymbol{\mathcal{J}})\rangle dt + \mathcal{O}(dt^2). \tag{2}$$

Large rotations are possible, but exceedingly rare. Their contribution to the expectation is negligible and we can work up to linear terms in dt. Now, for a centered Gaussian-distributed vector $\boldsymbol{x}$ of any dimension, the integration-by-parts identity $\langle f(\boldsymbol{x})x^\alpha\rangle = \sum_\beta\langle\partial f/\partial x^\beta\rangle\langle x^\beta x^\alpha\rangle$ holds [59]. Applying this identity and noting that U_n depends only on $\boldsymbol{\xi}_j$ for $j < n$ yields

$$\langle U_n\boldsymbol{\xi}_n\rangle\cdot\boldsymbol{\mathcal{J}} = \sum_{j<n}\left[\sum_{\alpha,\beta}\langle\xi_n^\alpha\xi_j^\beta\rangle\langle\tilde{\mathcal{R}}_0\cdots[\mathcal{J}_\beta\tilde{\mathcal{R}}_j]\cdots\tilde{\mathcal{R}}_n\rangle\mathcal{J}_\alpha\right]dt.$$

Substituting into Eq. (2) and reinterpreting the difference $(\langle U_{n+1}\rangle - \langle U_n\rangle)/dt$ as a derivative leads to

$$\frac{d}{dt}\langle U(0,t)\rangle = \sum_{\alpha,\beta}\int_0^t\langle U(0,t')\mathcal{J}_\beta\,U(t',t)\,\mathcal{J}_\alpha\rangle\langle\xi^\alpha(t)\xi^\beta(t')\rangle dt' - \langle U(0,t)\rangle\mathcal{K}^{\text{uncr}}. \tag{3}$$

The change of $\langle U(0,t)\rangle$ with time is due to the noise at time t. Noise uncorrelated with what has gone before tends to degrade memory of the past in a simple indiscriminate manner. But noise which is correlated with the past, as $\boldsymbol{\xi}$ is, has a more complicated effect. Since a Gaussian distribution is determined by its mean and covariance, the appearance of a simple covariance function in the governing equation (3) is a natural consequence.

Elegant as Eq. (3) is, it becomes difficult to work with in three or more dimensions since the matrices do not necessarily commute. Thus it does not give an autonomous evolution equation for $\langle U(0,t)\rangle$, as can be obtained in two dimensions. Some appropriate closure or approximation scheme is needed. However, the two-dimensional case is already very rich and many experimental studies involve self-propellers with an essentially two-dimensional motion due to a confining planar substrate. We therefore confine ourselves to the planar motion in the remainder of this paper. All rotations are about the z axis and the only matrices involved are

$$\mathcal{J}_z = \begin{bmatrix}0 & -1 & 0\\ 1 & 0 & 0\\ 0 & 0 & 0\end{bmatrix}, \quad \mathcal{P}_z^\perp = \begin{bmatrix}1 & 0 & 0\\ 0 & 1 & 0\\ 0 & 0 & 0\end{bmatrix}, \tag{4}$$

where $\mathcal{J}_z$ is the generator of infinitesimal rotation about the z-axis and $\mathcal{P}_z^\perp$ projects into the xy-plane. Since $\langle U(0,t)\rangle$ is written in terms of $\mathcal{P}_z^\perp$ and $\mathcal{J}_z$, and $[\mathcal{P}_z^\perp,\mathcal{J}_z] = \mathcal{P}_z^\perp\mathcal{J}_z - \mathcal{J}_z\mathcal{P}_z^\perp = 0$, the commutation $[U(t,t'),\mathcal{J}_z] = 0$ holds, and Eq. (3) yields an exact solution in terms of the autocorrelation of the Gaussian noise:

$$\langle U(0,t)\rangle = \exp[-\mathcal{K}^{\text{uncr}}t - \mathcal{F}_{\boldsymbol{\xi}}(t)\mathcal{P}_z^\perp] \tag{5a}$$

$$\mathcal{F}_{\boldsymbol{\xi}}(t) = \frac{1}{2}\int_0^t\int_0^t\langle\xi(t')\xi(t'')\rangle dt''dt'. \tag{5b}$$

By capturing the essential physics in the noise autocorrelation integral $\mathcal{F}_{\boldsymbol{\xi}}(t)$, the kinematrix treatment avoids the complication of dealing explicitly with probability distributions by extracting the necessary information solely from the noise autocorrelation function.

A swimmer's tail-to-head direction $\hat{\chi}$ coincides with its instantaneous direction of deterministic velocity $\hat{v}$ in a rectilinear motion. While such a swimmer usually moves *forward* along tail-to-head axis ($\hat{v} = \hat{\chi}$), it can also occasionally swim *backward* along the same axis ($\hat{v} = -\hat{\chi}$). We reference the instantaneous velocity to the tail-to-head direction by writing $\boldsymbol{v} \equiv v\hat{v} := v_s\hat{\chi}$. It is important to distinguish between v and v_s since the former is the speed (magnitude of the velocity) while the latter is a one dimensional velocity along the $\hat{\chi}$ axis such that for forward motion $v_s = v$ and for backward motion $v_s = -v$. As such, hereafter we refer to v_s as "signed-speed".

Now, choosing the laboratory frame such that $\hat{y} \equiv \hat{\chi}(0)$, the velocity pair correlator $\langle\boldsymbol{v}(0)\cdot\boldsymbol{v}(t)\rangle$, the ensemble average of displacement $\langle\Delta\boldsymbol{r}(t)\rangle$, the mean square displacement

$\langle|\Delta \boldsymbol{r}(t)|^2\rangle$, and effective diffusivity $D_{\rm eff}$ of the self-propeller can be obtained from

$$\langle \boldsymbol{v}(0)\cdot\boldsymbol{v}(t)\rangle = \langle v_s(0)v_s(t)\rangle\,\langle U(0,t)\rangle_{22}, \tag{6}$$

$$\langle \Delta \boldsymbol{r}(t)\rangle = \bar{v}_s\left[\int_0^t \langle U(0,t')\rangle dt'\right]\cdot\hat{\chi}(0), \tag{7}$$

$$\langle|\Delta \boldsymbol{r}(t)|^2\rangle = 2\int_0^t (t-t')\,\langle v_s(0)v_s(t)\rangle\langle U(0,t')\rangle_{22}dt', \tag{8}$$

and

$$D_{\rm eff} = \frac{1}{2}\int_0^\infty \langle v_s(0)v_s(t)\rangle\langle U(0,t')\rangle_{22}dt', \tag{9}$$

where the subscript "22" denotes a matrix element. If there is no backwards motion (for example, the commonly-studied case of constant speed), then the propagator can monitor the time evolution of the *dynamical* velocity vector rather than the *structural* tail-to-head vector. For such systems we make the modifications $v_s \mapsto v$ and $\hat{\chi} \mapsto \hat{v}$ in Eqs. (6)–(9).

The main contribution of this paper is extending the kinematic matrix theory to include Gaussian memory, as expressed by Eqs. (3)–(9). In the next section, as an example, we employ the formalism to discuss the physics of a rectilinear self-propeller with signed-speed fluctuation and Gaussian memory.

III. LINEAR MOTION WITH FLUCTUATING SPEED AND GAUSSIAN MEMORY

The interplay of multiple time scales of the elementary processes of motion determines different regimes of swimmer ensemble behavior, quantified by asymptotic effective diffusivity and mean-square-displacement. In this section we study a self-propeller subjected to velocity fluctuations and orientational inertia, such as appears in the upper left of Fig. 1. Velocity fluctuations lead to stochastic variation of speed, which may also have memory. The direction of motion may be influenced by stochastic noises arising from environmental fluctuations (e.g., Brownian kicks from fluid particles to a micron-sized self-propeller [41–43], spatially scattered food supply [60], or interaction with a substrate [61]) or internal fluctuations such as stochastic internal engine torque or decision-making processes of an organism.

Using a Fokker-Planck formalism, Peruani and Morelli [53] studied a self-propeller with speed fluctuation and Brownian orientational diffusion, which can account for internal engine fluctuations of biological systems. However, the lack of orientational inertia cannot capture the essential physics of self-propeller dynamics in many cases. For instance, Gautrais *et al.* [31] analyzed trajectories of *Kuhlia mugil* fish swimming in a tank, observing constant speed motion with persistent turns that cannot be modeled by a white noise. Rather, there was an inertia associated with the angular velocity leading to a decaying exponential autocorrelation. Correcting the white noise model with a finite inertial time leads to an Ornstein-Uhlenbeck process (OUP) for the angular velocity. Correspondingly, Gegond and Motsch [32] used a Fokker-Planck formalism to obtain the effective diffusivity of the fish with constant speed and OUP orientational dynamics. Their model [31,32] matches experimental data well, setting a solid ground for the presence of OUP dynamics in self-propeller dynamics. By adding a finite inertial time to a white noise, the OUP [62] serves as the simplest colored noise that not only shows success in self-propellers [31,32,63–68], but also applies to other fields of physics such as quantum processes [69–72], network dynamics [73], and genetics [74–76].

We analyze a more general model including both velocity fluctuations and orientational inertia, subsuming the results of [32,53], yet with less complexity and more intuitive connection to the self-propeller physics. The self-propeller moves in a plane at fluctuating velocity $\boldsymbol{v}(t) = v_s\hat{\chi}$ and with an orientation θ, defined by $\cos\theta = \hat{x}\cdot\hat{\chi}$ and $\sin\theta = \hat{y}\cdot\hat{\chi}$. The self-propeller's orientation changes according to

$$\frac{d\theta}{dt} = \xi, \tag{10}$$

in which ξ is a stationary OUP and η is Gaussian white noise of intensity $\tau_\xi^{-2}D_{\rm o}$:

$$d\xi/dt = -\tau_\xi^{-1}\xi(t) + \eta(t), \tag{11a}$$

$$\langle\eta(t)\eta(t')\rangle = 2\tau_\xi^{-2}D_{\rm o}\delta(t-t'), \tag{11b}$$

$$\langle\xi(t)\xi(0)\rangle = \tau_\xi^{-1}D_{\rm o}e^{-|t|/\tau_\xi}. \tag{11c}$$

Understanding the orientational wandering as being due to random torques, just as ordinary diffusion is due to random forces, this model takes into account the self-propeller's rotational inertia. The variance of the angular velocity, which may be a more convenient quantity for applications than $D_{\rm o}$, is simply $D_{\rm o}/\tau_\xi$. In the limit $\tau_\xi \to 0$, ξ acts as a white noise, recovering the simpler model of orientational Brownian motion diffusing at $D_{\rm o}$ with no inertia [53]. The autocorrelation integral [Eq. (5b)] for the OUP angular velocity ξ is monotonically increasing:

$$\mathcal{F}_{\boldsymbol{\xi}}^{\rm OUP}(t) = D_{\rm o}t + D_{\rm o}t\left[\frac{e^{-t/\tau_\xi}-1}{t/\tau_\xi}\right]. \tag{12}$$

The first term is the white-noise contribution and the second term is the modification due to inertia. Equations (5b), (10), and (12) yield the mean square angular displacement

$$\langle|\Delta\theta(t)|^2\rangle = 2\mathcal{F}_{\boldsymbol{\xi}}^{\rm OUP}(t) \approx \begin{cases} 2D_{\rm o}t & t \gg \tau_\xi \\ (t/\tau_\xi)D_{\rm o}t & t \ll \tau_\xi. \end{cases} \tag{13}$$

Here, τ_ξ is the crossover time from ballistic to diffusive angular dynamics. However, we shall see below that the physical regime of the ensemble behavior is governed not only by τ_ξ, but also the *disorientation time* τ_θ over which the orientation changes significantly: $\langle|\Delta\theta(\tau_\theta)|^2\rangle \sim 1$. As illustrated in Fig. 2, τ_θ can be distinct from both the orientational diffusion time $D_{\rm o}^{-1}$ and the inertial time τ_ξ. If the inertial timescale is very short ($\tau_\xi \ll D_{\rm o}^{-1}$), then the self-propeller "forgets" its prior orientation through pure diffusion and $\tau_\theta \sim D_{\rm o}^{-1}$. If the inertial time is large ($D_{\rm o}^{-1} \ll \tau_\xi$), then $\langle|\Delta\theta|^2\rangle$ becomes order one already in the ballistic regime and $\tau_\theta \sim (D_{\rm o}^{-1}\tau_\xi)^{1/2}$. Altogether, $D_{\rm o}\tau_\theta \sim \max(1, \sqrt{D_{\rm o}\tau_\xi})$. For example, the fish of [31] have $D_{\rm o}\tau_\xi \sim 1/2$.

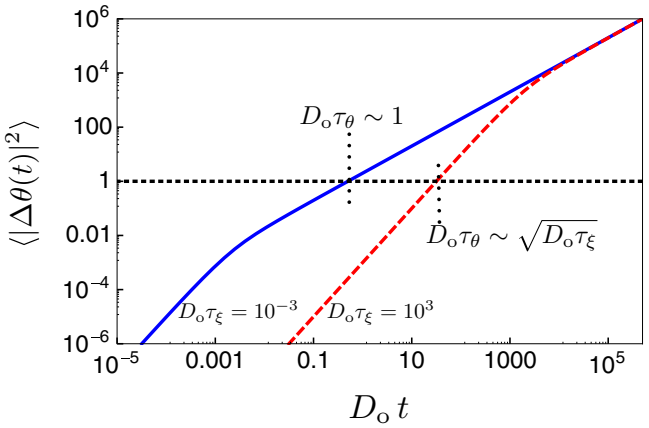

FIG. 2. (Color online) The disorientation time for a self-propeller to forget its initial orientation depends on the ratio of inertial τ_ξ and orientational diffusion D_o^{-1} time scales. If the $\tau_\xi \ll D_o$ we are close to the white noise limit and the self-propeller disorients over an orientational diffusion time scale $\tau_\theta \sim D_o^{-1}$. On the other hand, when the inertial time is much larger than the orientational time scale, the disorientation time is the geometric average of inertial and orientational diffusion time scales, $\tau_\theta \sim (\tau_\xi D_o^{-1})^{1/2}$.

Getting back to velocity fluctuations, a signed-speed autocorrelation function

$$\langle v_s(t)v_s(0)\rangle = \bar{v}_s^2 + \mathrm{var}(v_s)e^{-t/\tau_v} \tag{14}$$

appears naturally in many physical systems. It may arise from a self-propeller's interactions with the environment, varying terrain or fuel availability, and τ_v reflects the inertia associated with signed-speed relaxation. The use of signed-speed subsumes the ordinary speed (velocity magnitude) case where the motion is always directed along the tail-to-head direction, but also situations where the motion can sometimes be "backward". That might apply to crowded environments, such as for an individual cell in a cell monolayer [10–15]. If the dominance of forward over backward motion is slight, the dimensionless measure $\mathrm{var}(v_s)/\bar{v}_s^2$ of signed-speed fluctuations can be very large. In that case, we observe multiple crossovers in the mean-square-displacement curves, as will be discussed later. The form (14) may represent a biased OUP processes with mean $\bar{v}_s$. Alternatively, it may arise from internal engine fluctuations where the signed-speed jumps between discrete values. Such a case can be modeled by a Poisson distribution (at rate $1/\tau_v$) of "reset times" at each of which a new signed-speed is chosen independently from a fixed distribution with mean $\bar{v}_s$ and variance $\mathrm{var}(v_s)$. The path length between signed-speed resets has a mean $\bar{v}_s\tau_v$ and variance $\mathrm{var}(v_s)\tau_v^2$. For a self-propeller, a simple origin for such behavior might be a bistable engine, giving two possible values for v_s.

With the OUP autocorrelation integral (12) for persistent turning and the signed-speed autocorrelation function (14) thus motivated, we proceed to calculate the effective diffusivity D_{eff} of the self-propeller using Eqs. (5) and (9) as

$$D_{\mathrm{eff}} = \frac{\bar{v}_s^2}{2D_o}\Phi(D_o\tau_\xi,\infty) + \frac{\mathrm{var}(v_s)}{2D_o}\Phi(D_o\tau_\xi, D_o\tau_v), \tag{15}$$

where we have defined the dimensionless function Φ with the following physical limits:

$$\Phi(x,y) :\equiv \int_0^\infty \exp\{-x[e^{-z/x}-1]-z\}e^{-z/y}\,dz \tag{16a}$$

$$= e^x \sum_{k=0}^{\infty}(-x)^k \Big/ [k!\,(1+1/y+k/x)] \tag{16b}$$

$$\approx \begin{cases} e^x(1+1/y)^{-1}, & x \ll 1 \\ \left(\frac{\pi}{2}x\right)^{1/2}, & 1 \ll x \ll y^2 \\ y, & x \gg \max(1,y^2). \end{cases} \tag{16c}$$

The first term in the right-hand side of Eq. (15) describes the effective diffusion that would arise in the absence of signed-speed fluctuations, and the second term describes the unique contribution of signed-speed fluctuations to the effective diffusion. The reason for this clean separation is given below.

Figure 3 plots D_{eff} and Φ across a range of correlation times for orientation and speed. The diagram below facilitates an intuitive account of this behavior:

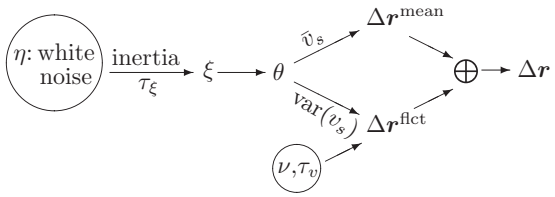

The self-propeller's signed-speed can be split into a mean and a fluctuation:

$$v_s(t) = \bar{v}_s + \sqrt{\mathrm{var}(v_s)}\,\nu(t), \tag{17}$$

where the noise ν obeys

$$\langle\nu(t)\rangle = 0, \quad \langle|\nu(t)|^2\rangle = 1. \tag{18}$$

The displacement can be similarly split as $\Delta\boldsymbol{r}(t) = \Delta\boldsymbol{r}^{\mathrm{mean}}(t) + \Delta\boldsymbol{r}^{\mathrm{flct}}(t)$. The diagram depicts the independent random inputs η and ν. Strictly speaking, $\Delta\boldsymbol{r}^{\mathrm{mean}}(t)$ and $\Delta\boldsymbol{r}^{\mathrm{flct}}(t)$ are not independent since they are driven by the same orientation process $\theta(t)$. But, they are *probabilistically orthogonal*, because the mean-speed and fluctuation-speed are: $\langle\nu(t)\rangle = 0$. As a result, $\Delta\boldsymbol{r}^{\mathrm{mean}}(t)$ and $\Delta\boldsymbol{r}^{\mathrm{flct}}(t)$ (and through them the mean signed-speed and signed-speed fluctuation) contribute to D_{eff} in a simple additive way.

Three major features of $\Phi(D_o\tau_\xi, D_o\tau_v)$ in Fig. 3(a) leap to the eye. First, $\Phi(D_o\tau_\xi,\infty)$, the curve for infinite $D_o\tau_v$ exhibits a crossover from a constant 1 to $\sim\sqrt{D_o\tau_\xi}$ at $D_o\tau_\xi \sim 1$. Second, for smaller values $1 \ll D_o\tau_v < \infty$, the curves follow that for $D_o\tau_v = \infty$ up to $D_o\tau_\xi \sim (D_o\tau_v)^2$, at which point they saturate to a value approximately $D_o\tau_v$. Finally, for very small speed correlation time $D_o\tau_v \ll 1$, $\Phi(D_o\tau_\xi, D_o\tau_v) \approx D_o\tau_v$ depends only weakly on $D_o\tau_\xi$. An intuitive physical interpretation of these observations and the asymptotics in Eq. (16c) follows from a comparison of the disorientation time τ_θ and speed correlation time τ_v. Henceforth, we use a more precise

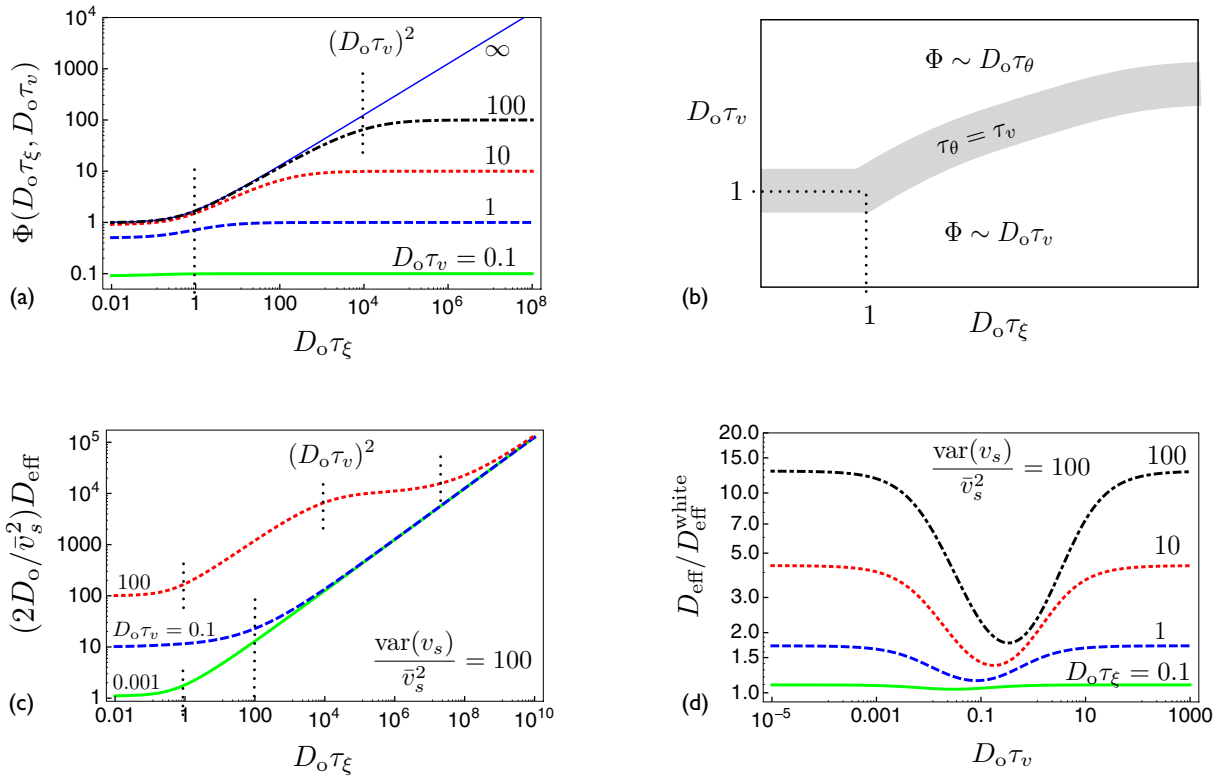

FIG. 3. (Color online) Effective diffusion coefficient $D_{\rm eff}$ of the linear self-propeller with orientational Gaussian noise characterized by correlation time τ_ξ, speed fluctuations characterized by correlation time τ_v and asymptotic orientational diffusion coefficient D_o. (a) The mean-speed and fluctuation speed make contributions to $D_{\rm eff}$ proportional to $\Phi(D_o\tau_\xi, \infty)$ and $\Phi(D_o\tau_\xi, D_o\tau_v)$, respectively. (b) Φ shows two major regimes depending upon whether the speed correlation time is smaller or larger than the disorientation time τ_θ. In the former case, the diffusion is essentially determined by speed fluctuations and in the latter by orientational wandering. The disorientation time τ_θ is proportional to $(D_o^{-1}\tau_\xi)^{1/2}$ when $D_o \ll \tau_\xi$, and saturates to ~ 1 as $D_o\tau_\xi \to 0$. (c) $D_{\rm eff}$ may contain several crossovers as a result of the relative sizes and individual crossovers of the mean-speed and fluctuation-speed components. Note that for $D_o\tau_\xi \gg [\mathrm{var}(v_s)/\bar{v}_s^2](D_o\tau_v)^2$, the mean-speed component always dominates. (d) Slices through $D_{\rm eff}$ in the other direction, normalized to the $D_o\tau_\xi = 0$ value.

definition for the disorientation time:

$$D_o\tau_\theta :\equiv \left[\max\left(1, \frac{\pi}{2} D_o\tau_\xi\right)\right]^{1/2}, \tag{19}$$

to recast Eq. (16c) into

$$\Phi(D_o\tau_\xi, D_o\tau_v) \approx \begin{cases} D_o\tau_v, & \tau_v \ll \tau_\theta \\ D_o\tau_\theta, & \tau_v \gg \tau_\theta. \end{cases} \tag{20}$$

Figure 3(b) reveals two regimes of this equation, showing $\tau_\theta \sim D_o^{-1}$ is independent of τ_ξ for $D_o\tau_\xi \ll 1$. A straightforward understanding of Eq. (20) is at hand. To better understand this behavior, we rewrite

$$\mathbf{\Gamma} := \Delta \boldsymbol{r}^{\rm fluc} \big/ \left[2D_o^{-1}\mathrm{var}(v_s)\right]^{1/2}, \tag{21a}$$

$$\Phi(D_o\tau_\xi, D_o\tau_v) = \lim_{t\to\infty} \frac{1}{t} \langle |\mathbf{\Gamma}(t)|^2 \rangle \tag{21b}$$

and analyze $\Phi(D_o\tau_\xi, D_o\tau_v)$ as the diffusive behavior of $\mathbf{\Gamma}$. In the limit $\tau_v \ll \tau_\theta$ where signed-speed changes very rapidly compared to orientation, the fluctuation part resembles a *one-dimensional* random walk along a slowly changing direction with step-duration $\Delta t = \tau_v$ and step-length-squared $\langle |\Delta \boldsymbol{r}^{\rm fluc}|^2 \rangle \approx \langle |\nu(t)|^2 \rangle \mathrm{var}(v_s)\tau_v^2$. By Eq. (18), $\Phi \approx \langle |\Delta \mathbf{\Gamma}|^2 \rangle / \tau_v \approx D_o\tau_v$. In the opposite limit, $\tau_v \gg \tau_\theta$, the fluctuation part has speed of order $\sqrt{\langle |\nu(t)|^2 \rangle \mathrm{var}(v_s)}$ which remains nearly constant during the time τ_θ, and resembles a two-dimensional random walker with step-duration τ_θ and step-length-squared $\langle |\Delta \boldsymbol{r}^{\rm fluc}|^2 \rangle = \mathrm{var}(v_s)\tau_\theta^2$. This leads to a ν-averaged diffusivity $\Phi \approx \langle |\mathbf{\Gamma}|^2 \rangle / \tau_\theta \approx D_o\tau_\theta$. Figure 3(a) now stands rationalized via Fig. 3(b) and Eq. (20).

Turning now to the interpretation of the more complicated behavior of the effective diffusivity (15) depicted in Fig. 3(c), we note that the various asymptotic regimes can be collected into

$$2D_{\rm eff} \sim \bar{v}_s^2 \tau_\theta + \mathrm{var}(v_s) \min(\tau_v, \tau_\theta). \tag{22}$$

The critical parameter determining the number of crossovers is $D_o\tau_v$.

If the orientational diffusion time scale greatly exceeds the speed correlation time ($\tau_v \ll D_o^{-1}$), we have $\min(\tau_v, \tau_\theta) = \tau_v$; the fluctuation-speed contribution $\mathrm{var}(v_s)\tau_v$ is independent of $D_o\tau_\xi$ and the only question is when this dominates the mean-speed contribution. In case $[\mathrm{var}(v_s)/\bar{v}^2]D_o\tau_v \ll 1$, the answer is never. This is exemplified by the solid green hockey-stick shaped curve in Fig. 3(c). Otherwise, there is a crossover from fluctuation-speed domination to mean-speed domination at $D_o\tau_\xi \simeq [\frac{\mathrm{var}(v_s)}{\bar{v}_s^2} D_o\tau_v]^2$, as shown in the blue dashed curve.

On the other hand, if the time required for changing signed-speed is much longer than the orientational diffusion time scale ($\tau_v \gg D_o^{-1}$), the story starts off similarly with a roughly constant value $2D_{\rm eff} \approx [\bar{v}_s^2 + {\rm var}(v_s)]D_o^{-1}$ up to about $\tau_\xi \sim D_o^{-1}$, at which point it shifts into the arm of the hockey stick with $2D_{\rm eff} \approx [\bar{v}_s^2 + {\rm var}(v_s)](D_o^{-1}\tau_\xi)^{1/2}$. But, when $D_o\tau_\xi$ exceeds $(D_o\tau_v)^2$, the mean-speed contribution continues to increase, while the fluctuation-speed contribution plateaus. If ${\rm var}(v_s)/\bar{v}_s^2 \gg 1$, this appears as a clear plateau, as seen in the dotted red curve of Fig. 3(c), until the mean-speed contribution becomes dominant at $\tau_\xi \sim D_o[\frac{{\rm var}(v_s)}{\bar{v}_s^2}\tau_v]^2$ and the $\sqrt{D_o\tau_\xi}$ behavior of the hockey stick returns.

Figure 3(d) gives another perspective on $D_{\rm eff}$ by slicing in the other direction and taking a ratio to the white noise limit ($D_o\tau_\xi \to 0$)

$$D_{\rm eff}^{\rm white} = \frac{\bar{v}_s^2}{2D_o} + \frac{{\rm var}(v_s)}{2D_o}\frac{1}{(1+1/D_o\tau_v)}. \tag{23}$$

In the limit $D_o\tau_v \to 0$ of rapid speed fluctuations the effective diffusivity depends only on average speed $D_{\rm eff} \sim \bar{v}_s^2\tau_\theta$, and as $D_o\tau_v \to \infty$, $D_{\rm eff} \sim [\bar{v}_s^2 + {\rm var}(v_s)]\tau_\theta$. In either extreme, $D_{\rm eff}$ is simply proportional to τ_θ, which is D_o^{-1} in the white noise limit. So, for *both* very large and very small $D_o\tau_v$, $D_{\rm eff}/D_{\rm eff}^{\rm white} \approx D_o\tau_\theta$, independently of the signed-speed parameters $\bar{v}_s$ and ${\rm var}(v_s)$. In between, if ${\rm var}(v_s)/\bar{v}_s^2$ is large enough, there is a region where $D_{\rm eff}$ is insensitive to $D_o\tau_\xi$ up to a large value. This corresponds to the long dashed blue plateau shown at $D_o\tau_v = 0.1$ in Fig. 3(c).

The effective diffusivity characterizes only the asymptotic behavior of the mean-square displacement. The full time dependence exhibits additional complexity. Using Eq. (8) we obtain the mean square displacement

$$\langle|\Delta\boldsymbol{r}(t)|^2\rangle :\equiv 4tD_{\rm eff} + 4t\,\frac{\bar{v}_s^2}{2D_o}\,\tilde{\Phi}(D_o\tau_\xi,\infty,D_o t) + 4t\,\frac{{\rm var}(v_s)}{2D_o}\,\tilde{\Phi}(D_o\tau_\xi,D_o\tau_v,D_o t), \tag{24}$$

where

$$\tilde{\Phi}(x,y,z) = \frac{e^x}{z}\sum_{k=0}^{\infty}\frac{(-x)^k[e^{-(1+1/y+k/x)z}-1]}{k!(1+1/y+k/x)^2} \tag{25a}$$

$$\approx \begin{cases} \frac{1}{2}z - \Phi(x,y), & z \ll \min(1,x,y) \\ 0, & z \to \infty. \end{cases} \tag{25b}$$

For times much shorter than all the characteristic time scales, $t \ll \min(D_o^{-1},\tau_\xi,\tau_v)$, we have ballistic motion $\langle|\Delta\boldsymbol{r}(t)|^2\rangle \approx [\bar{v}_s^2 + {\rm var}(v_s)]t^2$, independently of orientational, inertial and signed-speed correlation time scales. At very long times the self-propeller behaves diffusively; $\langle|\Delta\boldsymbol{r}(t\to\infty)|^2\rangle$ is $4tD_{\rm eff}$ and depends on all three time scales D_o^{-1}, τ_ξ and τ_v. Figure 4 shows the behavior of Eq. (24) in the limit of large speed fluctuations for a variety of time scales. Since $\langle|\Delta\boldsymbol{r}^{\rm mean}(t)|^2\rangle$ and $\langle|\Delta\boldsymbol{r}^{\rm flct}(t)|^2\rangle$ each has its own ballistic-to-diffusive crossover, in the limit of rapid, large signed-speed fluctuations, i.e., $D_o\tau_v \ll 1$ and ${\rm var}(v_s)/\bar{v}_s^2 \gg 1$, three clear crossovers are observed. We analyze the two limiting regimes $\tau_v \ll \tau_\theta$ and $\tau_\theta \ll \tau_v$. The mean-speed contribution $\langle|\Delta\boldsymbol{r}^{\rm mean}(t)|^2\rangle$ is

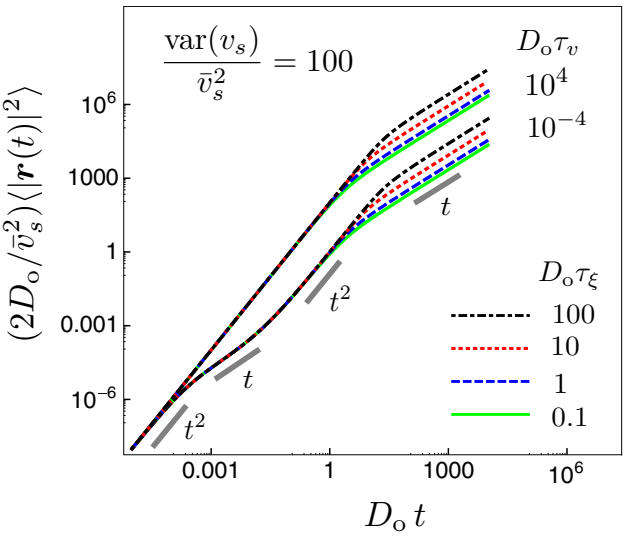

FIG. 4. (Color online) Mean-squared displacement of the linear self-propeller with Gaussian orientational noise of correlation time τ_ξ, signed-speed fluctuations with correlation time τ_v, and asymptotic orientational diffusion coefficient D_o. If the self-propeller disorients faster than signed-speed changes value, $\tau_\theta \ll \tau_v$, (upper curves) we observe a single crossover from ballistic to diffusive regimes at τ_θ; with increase in inertial time τ_ξ the crossover happens later. In the opposite regime $\tau_\theta \gg \tau_v$ (lower curves) for large signed-speed fluctuations ${\rm var}(v_s)/\bar{v}_s^2 \gg 1$ the signed-speed fluctuation contribution shows a one-dimensional ballistic to diffusive crossover about τ_v. Combined with mean signed-speed part (behaving like the $\tau_\theta \ll \tau_v$ case), this produces three crossovers.

invariably in the latter limit. Suppose first that the self-propeller disorients much faster than its signed-speed changes, i.e., $\tau_\theta \ll \tau_v$. Then, an individual self-propeller has a ballistic-to-diffusive crossover at time τ_θ. Its speed is stable over much longer times, so it behaves as though its diffusion coefficient were fluctuating on the time scale τ_v. On the other hand, if $\tau_v \ll \tau_\theta$, the fluctuation part of the displacement $[\Delta\boldsymbol{r}^{\rm flct}(t)]$ of an individual self-propeller has a ballistic-to-diffusive crossover at τ_v, but to a *nearly one-dimensional* diffusive motion since much before the self-propeller disorients, the signed-speed has changed many times. There is a second crossover, to genuinely two-dimensional diffusion, at τ_θ when the self-propeller starts to disorient. In either case, however, the ensemble average $\langle|\Delta\boldsymbol{r}^{\rm flct}(t)|^2\rangle$ will evidence only the primary crossover at $\min(\tau_\theta,\tau_v)$. When $\tau_\theta \ll \tau_v$ (the upper set of curves in Fig. 4), the full mean-square displacement exhibits just a single ballistic-to-diffusive crossover at τ_θ. In case $\tau_v \ll \tau_\theta$, the speed-fluctuation contribution $\Delta\boldsymbol{r}^{\rm flct}$ becomes diffusive earlier. If $\langle|\Delta\boldsymbol{r}^{\rm mean}(\tau_\theta)|^2\rangle/\tau_\theta \sim \bar{v}_s^2\tau_\theta \gg {\rm var}(v_s)\tau_v \sim \langle|\Delta\boldsymbol{r}^{\rm flct}(\tau_\theta)|^2\rangle/\tau_\theta$, the total motion can re-enter a ballistic regime when $\Delta\boldsymbol{r}^{\rm mean}$ comes to dominate somewhere between τ_v and τ_θ. Later, at τ_θ, this component, too, becomes diffusive. This is exemplified by the lower set of curves in Fig. 4.

IV. CONCLUDING REMARKS

The extension of kinematic matrix theory to incorporate correlated Gaussian noises expands its applicability to

real-world systems with significant inertia. The ability to work straightforwardly from just the noise autocorrelation simplifies calculations significantly and helps one to focus more on the physics of the problem. Our streamlined and close-to-the-physics treatment of the rectilinear self-propeller with velocity fluctuations and persistent turning—a model with real-world interest [32,53]—exemplifies this. This simplicity of kinematic matrix theory enables the study of more complicated systems with less mathematical sophistication, and provides a useful tool for experimentalists to develop models for analyzing their data.

We have treated here the case of exponentially decaying autocorrelations in Eqs. (11c) and (14). Correlations with asymptotic power-law decay have also been of great interest in recent years [77–79]. The methods used in this paper could also be applied with one or both of e^{-t/τ_ξ} in Eq. (11c) and e^{-t/τ_v} in Eq. (14) replaced by a power law $\sim t^{-\alpha}$ with $0 < \alpha < 1$. Power law correlations in ξ would lead to superdiffusive evolution of $\langle|\theta(t)|^2\rangle \sim t^{2-\alpha}$. But neither that nor power-law correlations in the speed would destroy asymptotic effective translational diffusion. Indeed, the extremes of a steady angular velocity or steady speed still result in effective diffusion. The effects are more subtle, and begin with the loss of the clear crossovers studied in Sec. III.

The general governing equation (3) applies also in higher dimensions where the simplifying feature of commutation of all the rotations disappears, and tractable approximation schemes remain to be found. Concrete development of the kinematrix approach to self-propellers moving in three dimensions will be a natural and useful direction for further study.

ACKNOWLEDGMENTS

This work was supported by the National Science Foundation under Grant No. DMR-0820404 through the Penn State Center for Nanoscale Science.

[1] P. Romanczuk, M. Bär, W. Ebeling, B. Lindner, and L. Schimansky-Geier, Eur. Phys. J. Spec. Top. **202**, 1 (2012).
[2] M. C. Marchetti, J. F. Joanny, S. Ramaswamy, T. B. Liverpool, J. Prost, M. Rao, and R. A. Simha, Rev. Mod. Phys. **85**, 1143 (2013).
[3] D. Chaudhuri, Phys. Rev. E **90**, 022131 (2014).
[4] V. Lobaskin, D. Lobaskin, and I. M. Kulic, Eur. Phys. J. Spec. Top. **157**, 149 (2008).
[5] H. C. Berg, Physics Today **53**, 24 (2000).
[6] G. Li, L.-K. Tam, and J. Tang, Proc. Natl. Acad. Sci. USA **105**, 18355 (2008).
[7] P. D. Frymier, R. M. Ford, H. C. Berg, and P. T. Cummings, Proc. Natl. Acad. Sci. USA **92**, 6195 (1995).
[8] M. Polin, I. Tuval, K. Drescher, J. P. Gollub, and R. E. Goldstein, Science **325**, 487 (2009).
[9] J. Saragosti, P. Silberzan, and A. Buguin, PLoS ONE **7**, e35412 (2012).
[10] M. Sadati, A. Nourhani, J. J. Fredberg, and N. Taheri Qazvini, WIREs Syst. Biol. Med. **6**, 137 (2014).
[11] D. Bi, J. H. Lopez, J. M. Schwarz, and M. L. Manning, Soft Matter **10**, 1885 (2014).
[12] R. M. Baker, M. E. Brasch, M. L. Manning, and J. H. Henderson, J. R. Soc. Interface **11**, 20140386 (2014).
[13] D. Selmeczi, L. Li, L. I. Pedersen, S. F. Nrrelykke, P. H. Hagedorn, S. Mosler, N. B. Larsen, E. C. Cox, and H. Flyvbjerg, Eur. Phys. J. Spec. Top. **157**, 1 (2008).
[14] D. Selmeczi, S. Mosler, P. H. Hagedorn, N. B. Larsen, and H. Flyvbjerg, Biophys. J. **89**, 912 (2005).
[15] D. Campos, V. Mendez, and I. Llopis, J. Theor. Biol. **267**, 526 (2010).
[16] L. Li, E. C. Cox, and H. Flyvbjerg, Phys. Biol. **8**, 046006 (2011).
[17] L. Li, S. F. Nørrelykke, and E. C. Cox, PLoS ONE **3**, e2093 (2008).
[18] P. J. M. Van Haastert and P. N. Devreotes, Nature Reviews Molecular Cell Biology **5**, 626 (2004).
[19] I. H. Riedel, K. Kruse, and J. Howard, Science **309**, 300 (2005).
[20] B. M. Friedrich and F. Jülicher, New J. Phys. **10**, 123025 (2008).
[21] A. Nourhani, Y.-M. Byun, P. E. Lammert, A. Borhan, and V. H. Crespi, Phys. Rev. E **88**, 062317 (2013).
[22] S. J. Ebbens and J. R. Howse, Soft Matter **6**, 726 (2010).
[23] J. R. Howse, R. A. L. Jones, A. J. Ryan, T. Gough, R. Vafabakhsh, and R. Golestanian, Phys. Rev. Lett. **99**, 048102 (2007).
[24] J. Wang and K. M. Manesh, Small **6**, 338 (2010).
[25] J. Gibbs and Y. Zhao, Front. Mater. Sci. **5**, 25 (2011).
[26] G. Theraulaz, E. Bonabeau, S. C. Nicolis, R. V. Sole, V. Fourcassie, S. Blanco, R. Fournier, J.-L. Joly, P. Fernandez, A. Grimal, P. Dalle, and J.-L. Deneubourg, Proc. Natl. Acad. Sci. USA **99**, 9645 (2002).
[27] E. Casellas, J. Gautrais, R. Fournier, S. Blanco, M. Combe, V. Fourcassie, G. Theraulaz, and C. Jost, J. Theor. Biol. **250**, 424 (2008).
[28] R. Jeanson, S. Blanco, R. Fournier, J. L. Deneubourg, V. Fourcassié, and G. Theraulaz, J. Theor. Biol. **225**, 443 (2003).
[29] H.-S. Niwa, J. Theor. Biol. **171**, 123 (1994).
[30] R. Mach and F. Schweitzer, Bull. Math. Biol. **69**, 539 (2007).
[31] J. Gautrais, C. Jost, M. Soria, A. Campo, S. Motsch, R. Fournier, S. Blanco, and G. Theraulaz, J. Math. Biol. **58**, 429 (2009).
[32] P. Degond and S. Motsch, J. Stat. Phys. **131**, 989 (2008).
[33] A. Ordemann, G. Balazsi, and F. Moss, Physica A: Statistical Mechanics and its Applications **325**, 260 (2003).
[34] N. Komin, U. Erdmann, and L. Schimansky-Geier, Fluc. Noise Lett **4**, L151 (2004).
[35] S. Bazazi, P. Romanczuk, S. Thomas, L. Schimansky-Geier, J. J. Hale, G. A. Miller, G. A. Sword, S. J. Simpson, and I. D. Couzin, Proc. Roy. Soc. B: Bio. Sci. **278**, 356 (2011).
[36] S. Bazazi, J. Buhl, J. J. Hale, M. L. Anstey, G. A. Sword, S. J. Simpson, and I. D. Couzin, Current Biology **18**, 735 (2008).
[37] A. M. Edwards, R. A. Phillips, N. W. Watkins, M. P. Freeman, E. J. Murphy, V. Afanasyev, S. V. Buldyrev, M. G. E. D. Luz, E. P. Raposo, H. E. Stanley, and G. M. Viswanathan, Nature **449**, 1044 (2007).
[38] D. Helbing, Rev. Mod. Phys. **73**, 1067 (2001).

[39] A. Aw, A. Klar, T. Materne, and M. Rascle, SIAM J. Appl. Math. **63**, 259 (2002).
[40] A. Nourhani, P. E. Lammert, A. Borhan, and V. H. Crespi, Phys. Rev. E **89**, 062304 (2014).
[41] S. Ebbens, R. A. L. Jones, A. J. Ryan, R. Golestanian, and J. R. Howse, Phys. Rev. E **82**, 015304 (2010).
[42] D. Takagi, A. B. Braunschweig, J. Zhang, and M. J. Shelley, Phys. Rev. Lett. **110**, 038301 (2013).
[43] A. Nourhani, P. E. Lammert, A. Borhan, and V. H. Crespi, Phys. Rev. E **87**, 050301(R) (2013).
[44] S. van Teeffelen and H. Löwen, Phys. Rev. E **78**, 020101(R) (2008).
[45] F. Schweitzer, W. Ebeling, and B. Tilch, Phys. Rev. Lett. **80**, 5044 (1998).
[46] M. E. Cates and J. Tailleur, EPL **101**, 20010 (2013).
[47] P. Romanczuk, I. D. Couzin, and L. Schimansky-Geier, Phys. Rev. Lett. **102**, 010602 (2009).
[48] P. Mandal and A. Ghosh, Phys. Rev. Lett. **111**, 248101 (2013).
[49] P. Hänggi and P. Jung, Adv. Chem. Phys. **89**, 239 (1995).
[50] M. M. Kłosek-Dygas, B. J. Matkowsky, and Z. Schuss, SIAM Journal on Applied Mathematics **48**, 425 (1988).
[51] M. San Miguel and J. M. Sancho, J. Stat. Phys. **22**, 605 (1980).
[52] A. Kamenev, B. Meerson, and B. Shklovskii, Phys. Rev. Lett. **101**, 268103 (2008).
[53] F. Peruani and L. G. Morelli, Phys. Rev. Lett. **99**, 010602 (2007).
[54] E. Lauga, W. R. Diluzio, G. M. Whitesides, and H. A. Stone, Biophys. J. **90**, 400 (2006).
[55] B. Steinberger, N. Petersen, H. Petermann, and D. G. Weiss, Journal of Fluid Mechanics **273**, 189 (1994).
[56] A. Cēbers and M. Ozols, Phys. Rev. E **73**, 021505 (2006).
[57] K. Ērglis, Q. Wen, V. Ose, A. Zeltins, A. Sharipo, P. A. Janmey, and A. Cēbers, Biophys. J. **93**, 1402 (2007).
[58] A. Cēbers, Journal of Magnetism and Magnetic Materials **323**, 279 (2011).
[59] D. Brydges, J. Frohlich, and T. Spencer, Commun. Math. Phys. **83**, 123 (1982).
[60] J. Strefler, W. Ebeling, E. Gudowska-Nowak, and L. Schimansky-Geier, Eur. Phys. J. B **72**, 597 (2009).
[61] C. Reichhardt and C. J. Olson Reichhardt, Phys. Rev. E **88**, 042306 (2013).
[62] G. E. Ornstein and L. S. Uhlenbeck, Phys. Rev. **36**, 679 (1930).
[63] C. Weber, P. K. Radtke, L. Schimansky-Geier, and P. Hänggi, Phys. Rev. E **84**, 011132 (2011).
[64] P. Dieterich, R. Klages, R. Preuss, and A. Schwab, Proc. Natl. Acad. Sci. USA **105**, 459 (2008).
[65] P. K. Radtke and L. Schimansky-Geier, Phys. Rev. E **85**, 051110 (2012).
[66] O. V. Yushchenko and A. Yu. Badalyan, Phys. Rev. E **85**, 051127 (2012).
[67] G. Szamel, Phys. Rev. E **90**, 012111 (2014).
[68] C. Torney and Z. Neufeld, Phys. Rev. Lett. **101**, 078105 (2008).
[69] M. K. Olsen, Phys. Rev. A **88**, 051802(R) (2013).
[70] M. Sarovar and M. D. Grace, Phys. Rev. Lett. **109**, 130401 (2012).
[71] J. Jing and T. Yu, Phys. Rev. Lett. **105**, 240403 (2010).
[72] H.-P. Stimming, N. J. Mauser, J. Schmiedmayer, and I. E. Mazets, Phys. Rev. Lett. **105**, 015301 (2010).
[73] Y. Hu, J. Trousdale, K. Josic, and E. Shea-Brown, Phys. Rev. E **89**, 032802 (2014).
[74] M. Assaf, E. Roberts, Z. Luthey-Schulten, and N. Goldenfeld, Phys. Rev. Lett. **111**, 058102 (2013).
[75] D. A. Charlebois, N. Abdennur, and M. Kaern, Phys. Rev. Lett. **107**, 218101 (2011).
[76] J. Berg, Phys. Rev. Lett. **100**, 188101 (2008).
[77] A. Clauset, C. R. Shalizi, and M. E. J. Newman, SIAM Review **51**, 661 (2009).
[78] E. P. Raposo, S. V. Buldyrev, M. G. E. da Luz, G. M. Viswanathan, and H. E. Stanley, J. Phys. A: Mathematical and Theoretical **42**, 434003 (2009).
[79] I. Eliazar and J. Klafter, Phys. Rep. **511**, 143 (2012).